Analysis of the mechanical transfer characterization between lodged sugarcane and the cutter by simulation modeling with UMAT subroutine

Tao Liu[1,2], Qingqing Wang[3], Jiaxun He[1,2], Dongbo Xie[1,2], Zhipeng Liu[1,2], Lichao Liu[1,2], Liqing Chen[1,2*]

(1. *College of Engineering, Anhui Agricultural University, Hefei 230036, China*;
2. *Anhui Intelligent Agricultural Machinery Equipment Engineering Laboratory, Hefei 230036, China*;
3. *Anhui Science and Technology University, Chuzhou 233100, Anhui, China*)

Abstract: Cutting the roots of sugarcane using cutters is a critical part of sugarcane harvesting, and the degree of breakage of the roots after cutting affects the germination and growth of sugarcane to a certain extent in the following year. However, the intricate interactions between the cutter and the stalk remain unclear. In order to fill this gap, this study first analyzed the conditions for no missed cuts during the operation of a double-disk cutter. Secondly, the research established a model of sugarcane stalk with anisotropy using the User-defined Material Mechanical Behavior (UMAT) subroutine based on the secondary development module of ABAQUS/Explicit. The cutting force curves obtained from simulation and test show a high correlation coefficient (R^2=0.9621), indicating the reliability of the model of sugarcane stalk in mechanical transfer. Subsequently, the simulation test of the blade rotating cutting characteristics in this study indicates that at a blade tilt angle of 11.3°, a blade rotating speed of 659.3 r/min, and a forward speed of 1.5 km/h, the maximum shear force on the blade is the largest, while the maximum cutting force is the smallest. Finally, based on the simulation results, this paper discussed the internal factors affecting the breakage rate of sugarcane stalks and predicted the damage location and damage force of the stalks by studying the stress wave transmission effect. Additionally, it analyzed the effects of single-knife cutting and multi-cutting on stalk incisions. The results indicated that multi-cutting causes more damage to the stalks and increases the breakage rate of sugarcane. The results of this study can provide a theoretical basis and technical reference for exploring the reduction of sugarcane residual cutting rate.

Keywords: sugarcane harvesting, UMAT, mechanical transfer characterization, cutter, simulation modeling
DOI: 10.25165/j.ijabe.20241703.8880

Citation: Liu T, Wang Q Q, He J X, Xie D B, Liu Z P, Liu L C, et al. Analysis of the mechanical transfer characterization between lodged sugarcane and the cutter by simulation modeling with UMAT subroutine. Int J Agric & Biol Eng, 2024; 17(3): 39–49.

1 Introduction

Sugarcane is an important cash crop, and many areas in China still rely on manual harvesting, which is costly, inefficient, and labor-intensive for farmers[1-4]. To solve these problems, introducing a sugarcane harvester has become a practical choice[5]. The cutter is a crucial component in the sugarcane harvester, and its operational performance directly affects the cutting quality of sugarcane. Existing sugarcane cutters have a significant degree of cutting breakage, which leads to the breakage of sugarcane ratoon regrowth branches, affecting the germination rate of regrowth branches in the following year, thus affecting the popularisation and application of sugarcane harvesters.

Domestic and foreign scholars have carried out many studies to solve the problem of poor cutting quality of sugarcane. Wang et al.[6] proposed a new counter-rotating base milling cutter with a support cut that can reduce the twisting and deformation of sugarcane ratoon stalks, thus reducing the rate of sugarcane ratoon. Momin et al.[7] studied four different shapes of base knives separately and showed that serrated blades have a minor effect on the cut quality. The conveying speed of the cane also has a significant influence on the quality of the stalk cut. To effectively minimize stem damage and juice loss, it is essential to maintain a steady and low conveyor speed. In addition, the proper overlap length of the upper blade and the lower blade help reduce cracks, splits, and chips[8]. Mo et al.[9] investigated the effect of axial vibration and frequency of sugarcane harvesters and related cutting parameters on cutting quality, laying the foundation for developing small sugarcane harvesters. Li et al.[10] established a virtual prototype of a sugarcane cutting system, investigated the effect of harvester and stalk cutting time under different forward and cutter speed conditions, and derived linear regression equations for cutter speed and forward time versus cutting time. Bai et al.[11] compared two cutting modes, above ground and below ground, and the results showed that the cutting

Received date: 2024-02-24 **Accepted date:** 2024-05-19
Biographies: Tao Liu, MS candidate, research interest: principles and theory of mechanics, Email: liutt@stu.ahau.edu.cn; **Qingqing Wang**, PhD candidate, research interest: modern agricultural machinery design and measurement, Email: wqq6322@163.com; **Jiaxun He**, MS candidate, research interest: modern agricultural machinery design and measurement, Email: hjxwj@stu.ahau.edu.cn; **Dongbo Xie**, PhD candidate, research interest: measurement and control technology for agricultural machinery, Email: dongbox@stu.ahau.edu.cn; **Zhipeng Liu**, MS candidate, research interest: principles and theory of mechanics, Email: liuzp@stu.ahau.edu.cn; **Lichao Liu**, PhD, Associate Professor, research interest: modern agricultural machinery design and measurement, Email: llchao@ahau.edu.cn.
***Corresponding author: Liqing Chen**, PhD, Professor, research interest: intelligent agricultural machinery design theory and technology. College of Engineering, Anhui Agricultural University, Hefei 230036, China. Tel: +86-13966658997, Email: lqchen@ahau.edu.cn.

force required to cut sugarcane in the below-ground cutting mode is smaller and more helpful in improving the cutting quality. In addition to cutting quality as an evaluation index, many scientists also consider cutting energy consumption and cutting loss as the basis for evaluating the quality of the cutter. Mathanker et al.[12] analyzed the effect of cutting speed and blade inclination on cutting energy and concluded that the specific cutting energy is directly proportional to the cutting speed. Wang et al.[13] discovered that the rotational speed of the cutter, the inclination of the cutter, and the diameter of the sugarcane positively influenced the cutting loss, while the feed rate of the sugarcane had a negative correlation with it. Research on sugarcane cutters at home and abroad mainly focuses on exploring the external factors affecting the quality of sugarcane cutting, including the cutter's motion parameters and design parameters. However, there are relatively few studies on the internal factors of cutting for sugarcane stalks.

Meanwhile, researchers employ the physical test method to assess the factors influencing the cutting quality of sugarcane. However, it is difficult to measure the internal stress distribution and damaged area of sugarcane stalks during the cutting process, and this kind of test requires the establishment of a specific scale of test platform, which is costly and has an extended test period. The finite element method (FEM) is a numerical method that engineers and scientists can utilize to solve complex mechanical problems by simplifying them and reducing the number of equations[14]. Wang et al.[15] established a finite element model of wild chrysanthemum using ANSYS Workbench and LS-DYNA software to study the effect of yield stress, breaking strain, and strain rate parameter C on the maximum shear force of straw. Niu et al.[16] established a simulation model of the olive branch using ANSYS software, which provided a vibrating harvester design as a reference basis. Liu et al.[17] established a three-point bending finite element model to study the cracking susceptibility of tomato pericarp during fruit development and post-harvest handling. These studies show that FEM can be used as a reliable method to determine the deformation behavior and stress distribution of biomaterials, so some scholars have investigated the cutting process of sugarcane by using the finite element method. Xie et al.[18] established a finite element model for the cutting process of sugarcane and analyzed the blade cutting resistance and stress distribution of sugarcane and blade during the cutting process. Qiu et al.[19] established a finite element model for the sugarcane-cutting process and effectively predicted the straw's damage location by analyzing the stalk's motion and the stress wave propagation.

In this study, a sugarcane stalk model was constructed considering anisotropic material properties using the UMAT subroutine within the secondary development module of ABAQUS, and an in-depth analysis of the mechanism of stalk cutting and breaking mechanism. The results provide a reliable basis for reducing the sugarcane ratoon rate and improving cutting quality.

2 Materials and methods

2.1 Sugarcane harvester machine structure and working principle

Figure 1 shows the composition and working principle of the hopper-type sugarcane harvester, which primarily includes a topper, crop dividers, base cutter, feed rollers, chopper rollers, extractors, and collection bin. The topper is responsible for removing the tips of the sugarcane, and the crop dividers separate the lodged and tangled sugarcane and raise it to a certain height. As the blade rotates, the double disc cutter removes the sugarcane roots. Subsequently, the feed rollers convey the sugarcane stalks to the chopper rollers, uniformly cutting them into sugarcane segments. Finally, the segments fall into the collection bin[20].

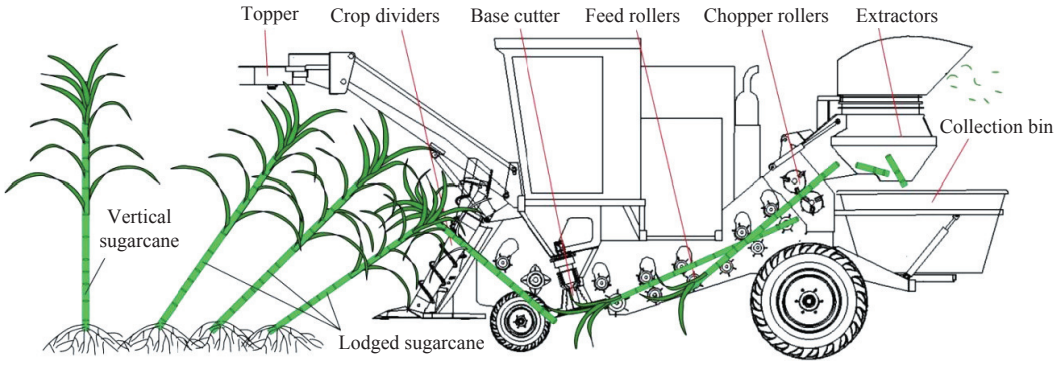

Figure 1 Sugarcane harvester systems

2.2 Mathematical modeling of double disc cutter dynamics

The double-disc sugarcane cutter is the primary cutting method used at present, and its cutter motion is a joint synthesis of rotary and horizontal forward motion. The operation schematic is shown in Figure 2.

Set the center of the disk for the origin of the coordinates O, horizontally to the right; that is, the cutter advances in the direction of the x-axis forward, vertically upward for the y-axis forward, the direction of the z-axis is perpendicular to the paper outwards, the blade on the line on the point a (the tip of the knife) the movement of the trajectory of the equation can be expressed as follows:

$$\begin{cases} x_a = R\cos(\omega t)\cos\varphi + vt \\ y_b = R\sin(\omega t) \\ z_c = R\cos(\omega t)\sin\varphi \end{cases} \quad (1)$$

where, x_a, y_a, z_a represent the three dimensional coordinates of point a on the blade, m; R is the radius of the blade apex, m; v is the forward speed of the cutter, m/s; ω is the rotational angular speed of the cutter, rad/s; φ is the tilt angle of the cutter disk, rad.

The condition that ensures no missed cuts by the cutter is that

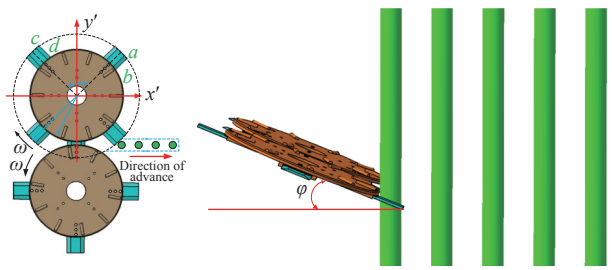

Figure 2 Diagram of the operation of a double disc cutter

there is no blank area between the motion trajectories formed by the blades on the cutter's cutter disk during cutting. The motion trajectory diagram of the knife blades is established in Figure 3 to explore the cutting trajectories of two neighboring knife blades. The shaded parts in the figure are the missed cuts of the cutting blades *ab* and *cd*.

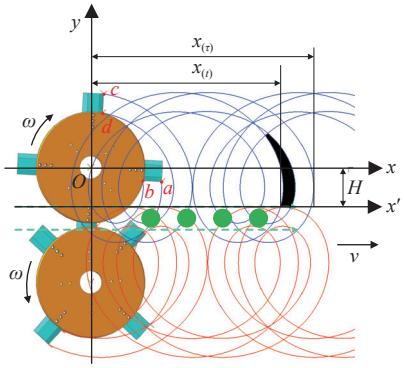

Note: $x_{(t)}$ represents the transverse coordinate displacement of point a on the blade, mm; $x_{(\tau)}$ represents the transverse coordinate displacement of point d on the blade, mm; *H* represents the distance between the center of the blade and the cane row, mm.

Figure 3 Diagram of the motion trajectories of two adjacent blades

In the *xoy* plane, the coordinates $y_a(t)$ of vertex *a* at moments *t* are equal to the coordinates $y_d(\tau)$ of endpoint *d* at moments *t*, i.e.

$$R\cos(\omega t) = r\cos(\omega t - \beta + \gamma) \tag{2}$$

where, γ is angle between the radial line at the apex of the blade and the radial line at the end of the blade, (°); *t* and τ represent the time, s; each pair of *t* and τ satisfying Equation (2) corresponds to an *x*-axis coordinate difference Δx.

$$\Delta x = v(\tau - t) + r\sin(\omega\tau - \beta + \gamma)\cos\varphi - R\sin(\omega t)\cos\varphi \tag{3}$$

To avoid leaky cuts, $\Delta x_{max} \leq 0$ needs to be satisfied. And to require Δx_{max}, Equation (4) needs to be differentiated and satisfied.

$$\begin{cases} \dfrac{\partial \Delta x}{\partial t} = 0 \\ \dfrac{\partial^2 \Delta x}{\partial t^2} < 0 \end{cases} \tag{4}$$

No missed cuts will occur when the sweeping trajectory of the double disc cutter blade completely covers the width of the row in which the sugarcane stalks are located. The motion of the double disc cutter is compounded by the motion of the two single disc cutters, and the no missed cuts are the same for both. Therefore, the general condition for the no missed cuts during the operation of the double disk cutter is:

$$\beta \leq \gamma + \arccos\left(\frac{k}{r\cos\varphi}\right) - \arccos\left(\frac{k}{R\cos\varphi}\right) + \cos\varphi\sqrt{\left(\frac{R}{k}\right)^2 - \frac{1}{\cos^2\varphi}} - \cos\varphi\sqrt{\left(\frac{r}{k}\right)^2 - \frac{1}{\cos^2\varphi}} \tag{5}$$

where, $k = v/\omega$, *k* represents the maximum speed ratio for non-missing cuts.

3 Sugarcane stalk-cutter finite element modeling and model verification

3.1 Finite element modeling of sugarcane stalk-cutter

Sugarcane is an anisotropic properties and complex material consisting of bark and core, and its modeling approach is critical to the accuracy of simulations. Most studies have simplified sugarcane into an elastic-plastic model with anisotropic properties. Although this simplification can provide a practical reference for the relationship between the blade and sugarcane stalk during the cutting process, it is difficult to comprehensively reproduce the relationship between the effects of various parameters between the blade and the stalk. Since it is difficult to accurately describe the material properties of actual sugarcane stalks with the intrinsic relationship model provided by the ABAQUS software, this study employed the user subroutine UMAT interface based on the secondary development module to create the required material intrinsic model and algorithm. UMAT allows the user to define the material's intrinsic relationship, and can perform calculations on materials not included in the ABAQUS material library, making the simulation more accurate and realistic[21].

To reduce computational complexity and facilitate modeling, the geometry of the stalk model was simplified by abstracting the sugarcane as a homogeneous cylinder. The cutter and sugarcane were modeled by 3D modeling software, and then their stp format was imported into the ABAQUS component module. A UMAT user subroutine was written using Fortran to define the cane skin and core material properties. There are many difficulties in measuring the mechanical properties of sugarcane due to the complexity of the microstructure of sugarcane itself and the limitations of the relevant instrumentation. In the current study, the material parameters of sugarcane mainly include the overall Poisson's ratio, Young's modulus, and shear modulus, which do not take into account the differences between the skin and core of sugarcane in terms of their mechanical properties nor the differences in the mechanical properties in different directions. In this paper, Poisson's ratio, Young's modulus, and shear modulus of sugarcane skin and core in different directions are obtained based on existing studies, and the material properties of sugarcane are listed in Table 1[18,22,23]. The diameter of the sugarcane stalk is 31.3 mm, and the thickness of the bark is 0.8 mm.

Table 1 Sugarcane material properties

Parameter	Sugarcane skin	Sugarcane core
Young's modulus E_X/MPa	1934	50
Young's modulus E_Y/MPa	1934	50
Young's modulus E_Z/MPa	1172	250
Poisson's ratio μ_{XY}	0.344	0.42
Poisson's ratio μ_{XZ}	0.314	0.35
Poisson's ratio μ_{YZ}	0.314	0.35
Shear modulus G_{XY}/MPa	11	17.6
Shear modulus G_{XZ}/MPa	446	92.8
Shear modulus G_{YZ}/MPa	446	92.8
Maximum tensile stress σ_X/MPa	47.02	47.02
Maximum compressive stress σ_X/MPa	101.4	101.40
Maximum tensile stress σ_Y/MPa	2.57	2.57
Maximum compressive stress σ_Y/MPa	4.45	4.45
Maximum tensile stress σ_Z/MPa	2.57	2.57
Maximum compressive stress σ_Z/MPa	4.45	4.45
Maximum shear stress σ_{XY}/MPa	2.25	2.25
Maximum shear stress σ_{XZ}/MPa	2.25	2.25
Maximum shear stress σ_{YZ}/MPa	2.25	2.25

The total length of the sugarcane stalk is 1000 mm. In simulating the case of roots in soil, the 100 mm at the lower end of the stalk is set as a fixed constraint. According to the actual production situation, the center point of the cutter disk was 220 mm from the ground. The inclination angle between the cutter disk and the ground ranges from 5° to 20°, and the spacing between the

cutter disk and sugarcane is modified according to the simulation requirements to ensure that the cutter disk can effectively cut sugarcane. The material of the cutting disk is commonly used 65 Mn, with a density of 7.85×10^3 kg/m^3, Young's modulus of 2.1×10^5 MPa, and Poisson's ratio of 0.3. The blade is 268 mm long and 90 mm wide, with a cutting angle of 16.5°, an effective cutting length of 80 mm, and the disk's diameter is 483 mm.

In the meshing module of ABAQUS, the sugarcane stalks were divided into a hexahedral mesh with C3D8R linear 3D stress mesh type. In order to improve the simulation efficiency and reduce the computation time, the mesh density was increased in the area where the stalks were cut with a mesh size of 1 mm×1 mm×1 mm, and the mesh size of the rest of the area was set to 1 mm× 1 mm×10 mm, and the total number of meshes divided is 143 360. Due to the complex shape of the cutter disk, it is divided into a wedge mesh C3D4 using the global seeding method. The approximate size of the global seeding is set to 10, and the total number of meshes is 72 580. The contact type between the blade and sugarcane stalk is face-to-face contact. The tangential behavior between the blades and the stalk is a penalized contact formula with a friction coefficient of 0.15. Figure 4 shows the established simulation model of the sugarcane stalk and the cutter.

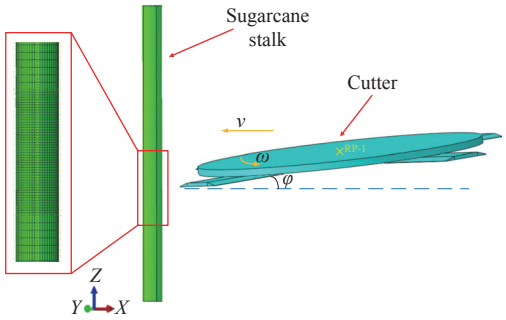

Figure 4 Simulation model of sugarcane-cutters

Since the simulation will produce large deformation and damage situations, the display dynamics analysis step is used here, and the output frequency is set to be the point-in-time output with a frequency of 2000. The irrelevant time points in the data output results are ignored to improve the efficiency of the simulation.

3.2 Model verification

A sugarcane shear test was conducted in this study to verify the accuracy of the developed finite element model of sugarcane. The equipment used for the test included an electronic universal testing machine (SANS) with a capacity of ±100 kN, a blade made of Mn material (length 150 mm; width 50 mm; thickness 4 mm; edge 30°), and two circular support blocks. In addition, Guangxi black-barked sugarcane was selected as the research object for the test, with a sample of uniform thickness, and the diameter of the sample at the proposed cutting position was measured using vernier calipers. The selected sugarcane stalks were characterized by a diameter of (39±0.5) mm and a length of 100 mm, with no apparent defects on the surface, and the epidermis was not damaged or cracked.

During the test, the sugarcane stalks were placed on two circular positioning blocks so that the distance between the two blocks was set to 10 mm. The cutting speed of the cutter of the controlled electronic universal testing machine was 100 mm/min, as shown in Figure 5a. Under the same conditions, the specimens were replaced, and the test was repeated 10 times. The computer records and generates the "load-displacement" relationship curve of each specimen shear test and finally calculates the average value of the 10 experiments. As shown in Figure 5b, the same shear test fixture model was established in ABAQUS software, keeping the same parameter settings as in the bench test, and the cutting speed of the cutter was also set to 100 mm/min.

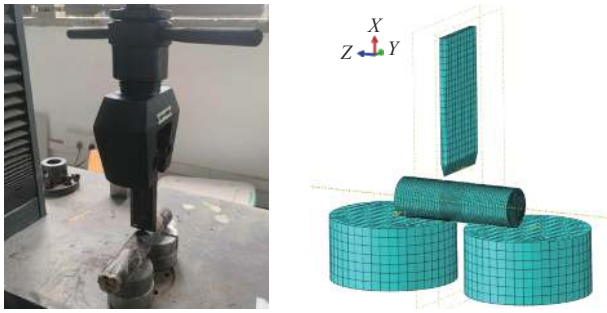

a. Bench test b. Finite element modeling of sugarcane stalk shear test

Figure 5 Sugarcane shear test

Figure 6 compares the "load-displacement" relationship curve from the bench test and the simulation curve. As seen from the curves, the simulation results show a similar trend to the test results. However, during the finite element analysis, as the tool erodes the mesh cells, the mesh cells disappear, resulting in a sudden disappearance of the tool force, which in turn causes fluctuations in the shear force and, ultimately, a significant jitter in the simulation curve. Notably, the experimental and simulation curves show a decreasing trend when the displacement reaches 1.2-1.5 mm. Since the sugarcane skin is stronger than the core, the two shear force curves decreased by 24.027 N and 72.877 N, respectively, when the skin was cut. Subsequently, with the increase of displacement, the shear force gradually increases. When the displacement reaches 30 mm, the shear force reaches the peak and then decreases. Using data processing software to analyze the data of the two shear force curves, the coefficient of determination R^2 between the experimental and simulated shear curves was obtained as 0.9621, which indicates that the experimental and simulated shear curves have a high degree of similarity in terms of fitting. The results of the validation tests show that the established finite element model of the sugarcane stalk is accurate and reliable for mechanical transfer applications.

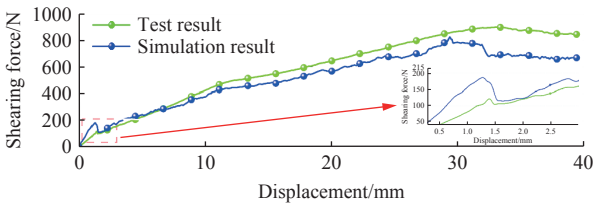

Figure 6 Sugarcane stalk shearing test results

4 Analysis of influencing factors

The cutting of sugarcane stalks mainly relies on the impact load generated by the high-speed rotation of the blade, which breaks through the yield limit of the stalks in an instant, thus realizing the cutting of sugarcane stalks[24]. The forces during the cutting process are shown in Figure 7, where the stalks are subjected to different cutting forces in the three directions *XYZ*, where the combined force is *F*, usually called the cutting force. In addition, the direction of the cutting force F_X is perpendicular to the axial direction of the stalk, which is the main component force leading to the cutting damage of the stalk, usually called shear force. Cutting and shear forces are necessary to ensure smooth stalk cutting. The lower the cutting

force, the less impact the impact will have on the sugarcane ratoon stalk, which reduces the broken rate of the sugarcane ratoon, resulting in a smoother cutting surface and less breakage[25]. In addition, the higher the shear force, the lower the broken rate of sugarcane ratoon.

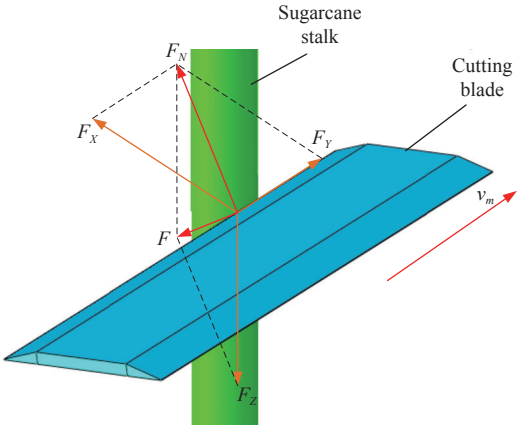

Note: F_X, F_Y, and F_Z represent the different cutting forces on the stalks in all three directions of *XYZ*, N; F_N represents the combined force in the *X* and *Y* directions, N; *F* is the combined force of the three directional forces, N.

Figure 7 Force analysis of the sugarcane stalk-cutting process

4.1 Analysis of the influence of cutter inclination angle on stem cutting

When the angle formed between the blade and the horizontal ground is φ, the force of the blade cutting the stalk is shown in Figure 8, at which time sugarcane is subjected to the force F_N in the direction of the perpendicular blade and the force F_T in the direction of the parallel blade, and the speed of the blade can be divided into the same direction of v_n and v_t. With the increase in the inclination angle of the blade, the speed of the blade in the perpendicular direction increases, which improves the resistance to cutting the fibers of the stalks and consequently reduces the maximum value of the shear force and reduces the broken rate of sugarcane stalks.

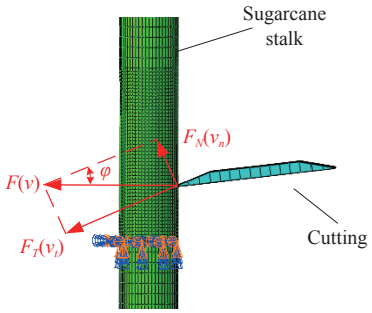

Figure 8 Force analysis of blade inclination angle

Figure 9 shows the magnitude of shear and cutting forces on the cutter for cutting sugarcane stalks at different blade inclination angles during multi-cutting. From the curves in the figure, it can be observed that with the increase of the blade inclination angle, the maximum shear force and the maximum cutting force on the blade show a decreasing and then increasing trend. The maximum shear force and the maximum cutting force reached the maximum value when the tilt angle of the cutter disk was 20°, and the maximum values were 133.1 N and 471.1 N.

4.2 Analysis of the influence of cutter rotation speed and forward speed on stem cutting

According to the analysis of the cutter motion, it can be seen that changes in the value of the cutting speed ratio *k* (the ratio of the forward speed of the harvester to the rotational speed of the cutter) significantly affect the trajectory of the blade, and at the same time has an impact on the shear force generated by the blade during the stalk cutting process. Figure 10 shows the decomposition of the velocity of motion of the apex *P* of the blade at a given moment. From the figure, it can be observed that the vertex *P* has a parallel velocity v_m along the blade in the horizontal direction and a rotational linear velocity v_R perpendicular to the direction of the blade, with $v_R = \omega R$, resulting in a resultant velocity of *v*. The angle between the resultant velocity and the linear velocity is $\angle vPv_R$. When the forward velocity increases to v'_m , the rotational linear velocity decreases to v'_R, and at this point, the resultant velocity is v', and the angle between the resultant velocity and the linear velocity is $\angle v'Pv'_R$. The figure shows that the angle $\angle v'Pv'_R$ is larger than the angle $\angle vPv_R$, and the combined velocity v' is shifted horizontally, which decreases the blade's shear force to cut the stalks. At the same time, as the velocity v'_m increases, the sugarcane ratoon shear force acting in the direction of the line velocity decreases. The thrust force along the blade direction tends to increase, which in turn leads to an increase in the thrust force in the parallel direction of the blade on the stalk and a decrease in the shear force in the perpendicular direction of the blade, which enhances the tendency of the sugarcane ratoon to be pushed off instead of being cut off typically, leading to an increase in sugarcane ratoon breakage. Based on the above analysis, it can be seen that an increase in the speed ratio *k* leads to an increase in the broken rate of sugarcane ratoon.

$$\begin{cases} k = \dfrac{v_m}{\omega} \\ v_R = \omega R \end{cases} \tag{6}$$

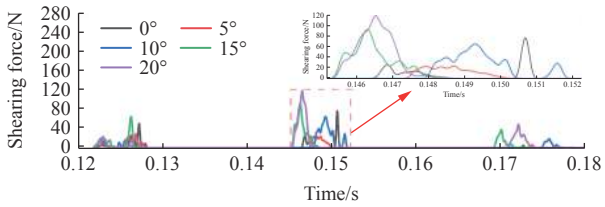

a. Shear force curve of sugarcane stem cutting with different inclination cutters

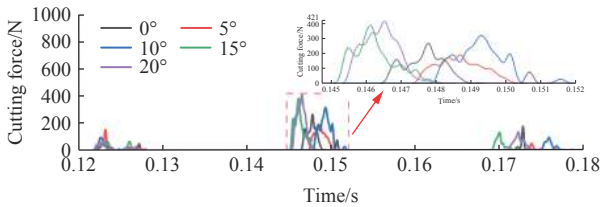

b. Cutting force curve of sugarcane stem cutting with different inclination cutters

Figure 9 Effect of different blade inclination angles on shear and cutting forces

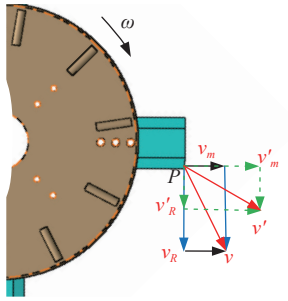

Figure 10 Blade vertex velocity analysis graph

Figure 11 shows the cutter's shear force and cutting force curves for cutting sugarcane stalks when the rotational speed of the cutter is varied in the range of 400-800 r/min during multi-cutting. It can be observed from the curves in the figure that the maximum shear force shows a trend of increasing and then decreasing with the increase of the rotational speed of the cutter disk, and the maximum shear force reaches the maximum value of 128.26 N at the rotational speed of the cutter disk of 600 r/min. In contrast, the maximum cutting force shows a trend of increasing, then decreasing, and then increasing, and when the rotational speed of the cutter disk reaches 700 r/min, the maximum cutting force reaches the maximum value, and the maximum value is 346.7 N.

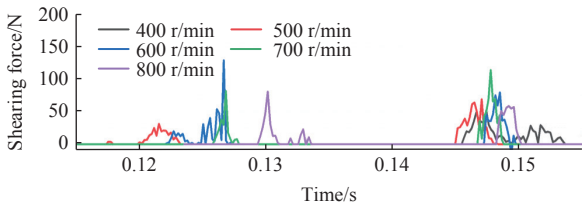

a. The curve of the shear force with the rotation speed of the cutter

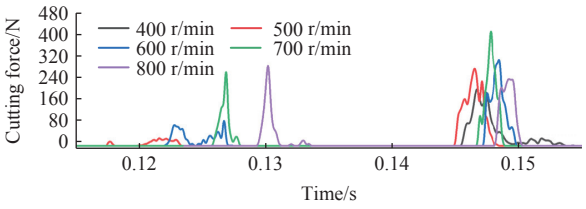

b. The curve of the cutting force with the rotation speed of the cutter

Figure 11 Effect of different blade speeds on shear and cutting forces

Figure 12 shows the shear and cutting forces of the cutter when cutting sugarcane stalks at a forward speed of 1-4 km/h during multi-cutting. Due to the different forward speeds set for each simulation, there is a difference in the time taken for the cutter to reach the sugarcane stalks at the same position, and therefore, the time taken by the cutter to cut the stalks is also different. When the forward speed reaches 3.4 km/h, the maximum shear force and the maximum cutting force on the sugarcane stalks reach the maximum value, which is 289.6 N and 645.4 N, respectively, and the maximum shear force and the maximum cutting force on the sugarcane stalks show a tendency of increasing and then decreasing with the increase of the forward speed. When the forward speed is 1 km/h, the shear force and cutting force generated by the cutter each time it cuts sugarcane stalks change less.

4.3 Orthogonal test

4.3.1 Experimental design

The cutting knife's rotational speed and tilt angle significantly affect stem fracture. Combined with the analysis of the influencing factors, the tilt angle of the cutting knife, the forward speed, and the rotational speed of the cutting knife are chosen as the experimental factors, and the range of experimental parameters was determined according to the actual operation process and the results of related scholars' research[7,19,26], and also the maximum cutting force and the maximum shear force are chosen as the evaluation indexes, and the coding table of the level of orthogonal test is listed in Table 2.

4.3.2 Test result

According to the orthogonal test table in Table 2, the simulation test results under different combinations were obtained using data analysis software, as listed in Table 3. In the table, Y_1 represents the maximum shear force for stem cutting, and Y_2 represents the maximum cutting force during sugarcane cutting.

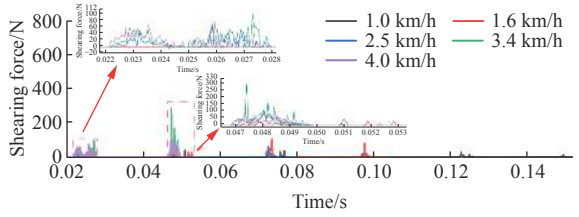

a. Shear force curves of sugarcane stalk at different forward speeds

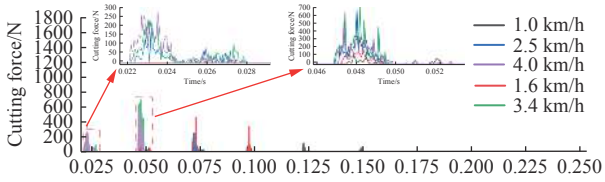

b. Cutting force curve of sugarcane stalk at different forward speeds

Figure 12 Effect of different forward speeds on shear and cutting forces

Table 2 Orthogonal test level coding table

Code	Factors		
	X_1	X_2	X_3
1.682	20	700	4
+1	17	660	3.4
0	12.5	600	2.5
–1	8	540	1.6
–1.682	5	500	1

Note: X_1 represents the blade inclination angle, (°); X_2 represents the blade speed, r/min; X_3 represents the forward speed, km/h.

Table 3 Test combination and results

Test	Factors			Index	
	X_1	X_2	X_3	Y_1/N	Y_2/N
1	1	1	–1	281.831	353.763
2	0	0	–1.682	382.662	447.681
3	1.682	0	0	365.818	584.911
4	0	0	0	309.634	411.721
5	0	1.682	0	271.601	356.545
6	–1.682	0	0	332.117	452.272
7	0	–1.682	0	289.416	401.498
8	1	–1	1	238.874	319.908
9	–1	–1	1	217.681	358.779
10	0	0	0	221.884	257.865
11	–1	1	1	206.103	260.712
12	0	0	0	221.314	256.207
13	1	–1	–1	372.445	542.052
14	0	0	0	225.127	285.872
15	–1	–1	–1	278.629	385.801
16	0	0	1.682	173.373	262.794
17	1	1	1	267.978	326.257
18	–1	1	–1	329.943	441.29
19	0	0	0	258.634	326.255
20	0	0	0	198.363	289.558

Based on the data samples in Table 3, the quadratic polynomial regression model equations for the two models of maximum shear force and maximum cutting force were obtained using the data analysis software:

$$Y_1 = 240.19 + 13.58X_1 - 3.79X_2 - 50.10X_3 - 12.66X_1X_2 + 4.67X_1X_3 + 7.10X_2X_3 + 32.03X_1^2 + 7.84X_2^2 + 6.96X_3^2 \quad (7)$$

$$Y_2 = 306.22 + 23.32X_1 - 21.97X_2 - 56.25X_3 - 17.42X_1X_2 - 5.26X_1X_3 + 5.14X_2X_3 + 64.91X_1^2 + 15.58X_2^2 + 7.17X_3^2 \quad (8)$$

According to the ANOVA of the regression model (Table 4 and Table 5), the following conclusions can be drawn: the Y_1 and Y_2 models ($p<0.05$) were significant, lack of fit term ($p>0.05$) was not significant, which indicated that the test data and regression model were fitted to a high degree. The test factors with primary and secondary effects on maximum shear were forward speed > cutter inclination > cutter rotational speed, where forward speed was highly significant, the self-intersecting term for cutter rotational speed was highly significant, and the other interaction and self-intersecting terms were not significant; The primary and secondary factors of the test factors on the maximum cutting force were forward speed > cutter tilt angle > cutter rotational speed, where forward speed was significant, the self-crossing term for cutter tilt angle was highly significant, and the other terms were not significant.

Based on the analytical results of the regression model, 3D response surface plots of the interaction effects between the factors were generated using data analysis software. The interaction effect of the blade inclination angle and the blade rotational speed on the maximum shear force, when the forward speed is 2.5 km/h, is shown in Figure 13a. When the blade inclination angle is approximately greater than 0 level, the maximum shear force shows an increasing trend with the increase of the blade rotational speed; when the blade inclination angle is approximately less than 0 level, the maximum shear force shows a decreasing trend with the increase of the blade rotational speed; when the blade inclination angle is gradually increased, the maximum shear force decreases first and then increases. Figure 13b demonstrates the interactive effect of the cutter tilt angle and forward speed on the maximum cutting force at a cutter speed of 600 r/min. The maximum shear force decreases and increases as the cutter tilt angle increases; the maximum shear force decreases as the forward speed increases. In Figure 13c, the interaction effect of the blade rotational speed and the forward speed on the maximum cutting force when the blade inclination angle is 12.5° demonstrates that the maximum shear force decreases with the increase of the forward speed; when the forward speed is approximately less than 0.5 level, the maximum shear force tends to increase with the decrease of the blade rotational speed; and when the forward speed is approximately greater than 0.5 level, the maximum shear force shows a decreasing trend.

Table 4 ANOVA variance analysis of test factors on maximum shear force

Source	SS	df	MS	F	p
Model	1.221E+05	9	13 561.76	3.10	0.0462*
X_1	7427.03	1	7427.03	1.70	0.2216
X_2	6595.09	1	6595.09	1.51	0.2474
X_3	43 210.32	1	43 210.32	9.89	0.0104*
X_1X_2	2427.72	1	2427.72	0.5554	0.4733
X_1X_3	221.03	1	221.03	0.0506	0.8266
X_2X_3	210.97	1	210.97	0.0483	0.8305
X_1^2	60 750.27	1	60 750.27	13.90	0.0039**
X_2^2	3500.04	1	3500.04	0.8007	0.3919
X_3^2	742.08	1	742.08	0.1698	0.6890
Residual	43 709.66	10	4370.97	--	--
Lack of Fit	26 662.77	5	5332.55	1.56	0.3177
Pure Error	17 046.89	5	3409.38	--	--
Cor Total	1.658E+05	19	--	--	--

Note: SS represents the sum of squares, df represents degrees of freedom, MS represents the mean sum of squares, * represents that the item is significant ($0.01<p<0.05$), ** represents that the item is exceptionally significant ($p<0.01$), and the same below.

Table 5 ANOVA of test factors on maximum cutting force

Source	SS	df	MS	F	p
Model	54 126.04	9	6014.00	3.57	0.0301*
X_1	2518.21	1	2518.21	1.49	0.2496
X_2	195.99	1	195.99	0.1163	0.7402
X_3	34 278.12	1	34 278.12	20.34	0.0011**
X_1X_2	1281.34	1	1281.34	0.7602	0.4037
X_1X_3	174.51	1	174.51	0.1035	0.7543
X_2X_3	403.65	1	403.65	0.2395	0.6351
X_1^2	14 794.29	1	14 794.29	8.78	0.0142*
X_2^2	885.31	1	885.31	0.5253	0.4852
X_3^2	697.54	1	697.54	0.4139	0.5345
Residual	16 854.88	10	1685.49	--	--
Lack of fit	9030.79	5	1806.16	1.15	0.4394
Pure error	7824.08	5	1564.82	--	--
Corr total	70 980.92	19	--	--	--

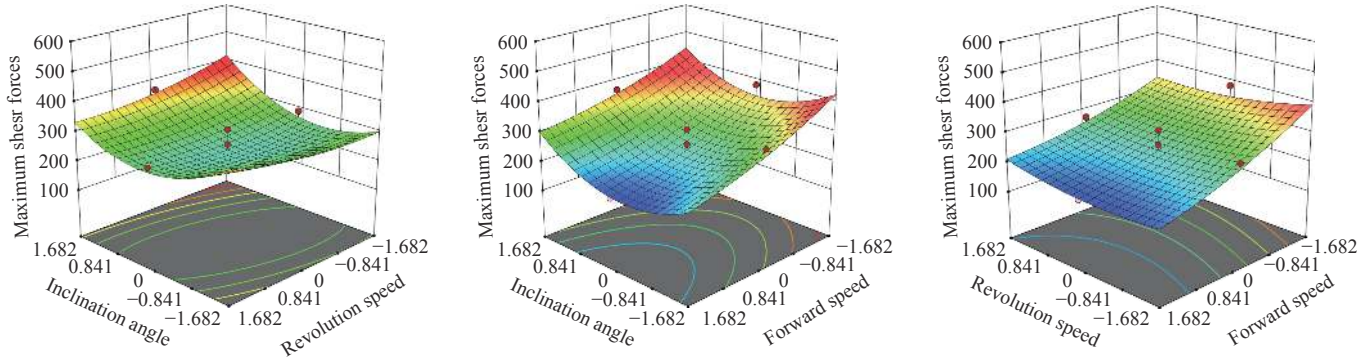

a. X_1X_2 b. X_1X_3 c. X_2X_3

Figure 13 Two-factor response surface to maximum shear force

Within the selected parameter range, the effect of the interaction between the test factors on the maximum cutting force is shown in Figure 14, and the overall trend of the response surface is similar to that of the maximum shear force. When the forward speed is 2.5 km/h, Figure 14a shows the effect of the interaction between the blade inclination angle and the blade speed on the maximum cutting force. With the gradual increase of the blade inclination angle, the maximum cutting force of the stalk shows a trend of decreasing and then increasing; when the coded value of the blade inclination angle is more significant than –0.8, the maximum cutting force shows a decreasing trend with the increase of the blade rotational speed; and in the case that the coded value of blade inclination angle is less than –0.8, the maximum cutting force shows an increasing trend with the increase of the blade rotational speed. Figure 14b shows the interactive effect of the cutter tilt angle and forward speed on the maximum cutting force at a cutter speed of 600 r/min. With the increase of the tilt angle of the cutter disk, the maximum cutting force first decreases and then gradually increases; with the increase of the forward speed, the maximum cutting force slowly decreases. At a cutter tilt angle of 12.5°, Figure 14c reveals the trend of maximum cutting force under the interaction of cutter rotational speed and forward speed. The maximum cutting force gradually decreases with the increase of cutter blade speed and forward speed.

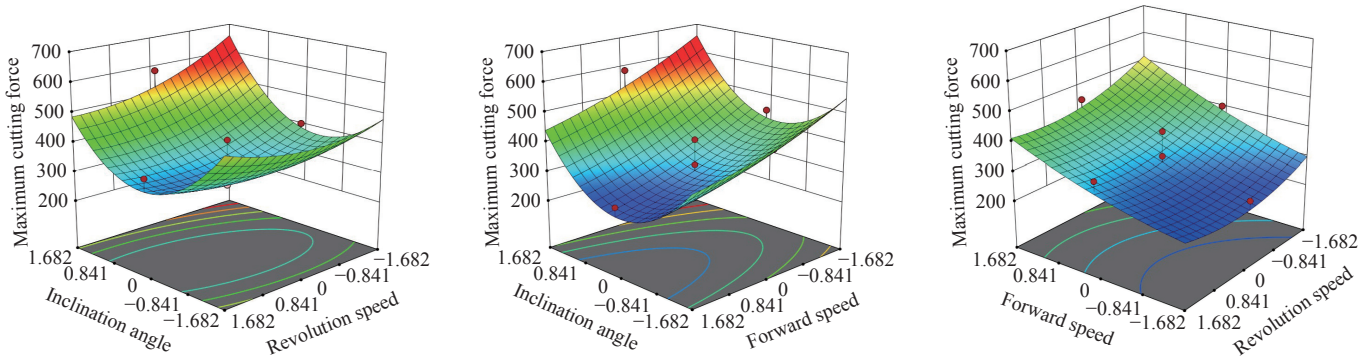

a. X_1X_2 b. X_1X_3 c. X_2X_3

Figure 14 Two-factor response surface for maximum cutting force

According to the above regression model, the optimal parameters obtained by solving the regression model using the data analysis software with the values of decreasing the maximum cutting force and increasing the maximum shear force are 11.3° of cutter tilt angle, 659 r/min of cutter rotational speed, and a forward speed of 1.5 km/h. The maximum shear and cutting forces are 305.102 N and 368.147 N, respectively.

4.3.3 Variation of cutting forces in different directions

According to the optimal parameter combinations obtained from orthogonal experiments, the finite element simulation of single-knife cutting stalks for sugarcane was carried out. The change curves of the extraction cutting force in the three directions of X, Y, and Z are shown in Figure 15. The direction of the Y axis is the same as the forward direction of the cutter, and the blue curve in the figure represents its cutting force; the red curved surface depicts the cutting force in the X direction, whose direction is perpendicular to the axial direction of the stalk, and the trend of the change is approximately equal to the axial cutting force of the knife plate, which is also known as the shear force. The cutting force in the Z direction is along the axial direction of the stalk, shown by the figure's blue curve. According to Figure 15 can be obtained, the trend of its change is more similar to the cutting force, and the overall trend of the size of the exact moment is F_X>F_Y>F_Z, which also indicates that the shear force F_X has the most significant impact on the cutting of stalks, and increasing the shear force is conducive to improving the efficiency of the cutting of stalks and the cutting quality of sugarcane ratoon. The increase of shear force can improve the ability to overcome the axial load of stalks, thus reducing the risk of being pulled apart and broken during the cutting process of sugarcane ratoon, which can effectively reduce the degree of breakage of sugarcane ratoon and improve the overall quality of cutting, thus reducing the broken rate of sugarcane ratoon.

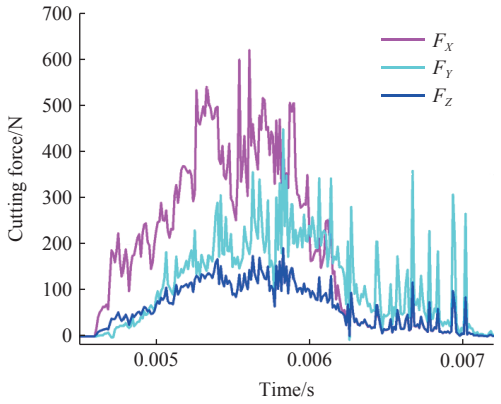

Figure 15 Cutting force variation in different directions

5 Results and discussion

5.1 Stress wave transmission

When a solid material is subjected to a time-dependent external load, the motion process always involves force wave transmission and reflection interactions[27]. When the blade cuts the front surface of the sugarcane, the cutting force perturbation gradually propagates from near to far end in the sugarcane body, forming a force wave. Figure 16 shows the stress wave transmission of the blade as it cuts the sugarcane stalk under the action of high-speed rotation.

When the stalk is loaded, its force transfer effects and interactions mainly go through four stages. When the blade touches the sugarcane stalk, only a tiny part of the incision is affected, and the force wave transfer shows a gradual diffusion in the form of a circular arc, with the maximum extending to half of the cross-section of the stalk, which exhibits a tendency of gradual decrease along the incision and outward. As the blade penetrates deeper into the stalk, the back of the stalk incision is subjected to the reaction forces transmitted by the stress wave, creating a locally pressurized area. The pressure wave in this region is relatively small, and all

manifested in the transmission to the root and upper part of the stalk. Due to the cutting force and stress wave transmission, the cutting section and back of the axial stalk are unbalanced, resulting in tensile loads in the axial direction of the stalk[28]. As the blade cuts more profoundly, the lateral pressure area gradually decreases, and eventually, the pressure wave at the incision disappears after the stalk is completely cut off. At this time, the stress wave transmission is mainly dispersed along the axial direction of the incision, and the transmission effect is distributed to the whole sugarcane stalk, increasing the axial tensile load. When the sugarcane stalk is completely cut, the stress wave transmission is transmitted along the stalk's axial direction, and the local stress at the incision is more concentrated, which gradually disperses and decreases along the diffusion direction.

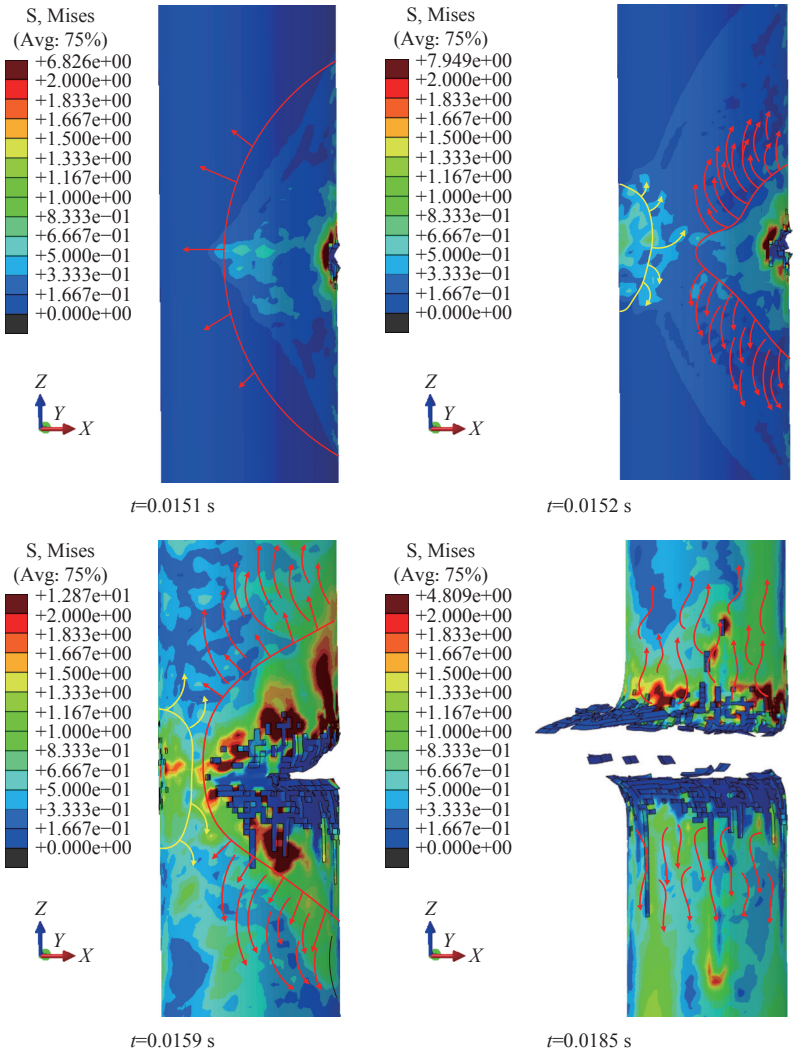

Figure 16 Blade epidermal to completely cut stalk stress transfer

The above analysis reveals that the cutting stress generates tensile load primarily distributed in the axial direction on the incision site, while compressive stress is predominantly distributed on the back side of the stalk incision. The variation of tensile stress directly affects the cutting breakage of the stalk. When the tensile load generated by the cutting stress is large, the local stress in the stalk incision is more concentrated and gradually disperses and decreases along the axial direction. Before sugarcane stalks are entirely cut, tensile and compressive stress waves converge at the incision location, and since the tensile loads are more significant than the compressive loads, the stalks are susceptible to damage, especially during multi-knife cutting, which may include rupture of the cane skin and splitting of the stalks. The effect of tensile forces affects not only the breakage at the incision but also the roots of the stalks. As the tensile load increases during the cutting process, the pull on the roots of the stalks also increases, which may result in the loosening of the roots of sugarcane stalks, which may drag the roots of sugarcane out of the soil after exceeding the load of interaction between the roots of the stalks and the soil.

5.2 Stem incision analysis

The changes in the incision of the upper and lower sugarcane segments during the process of the sugarcane stalks being cut by the cutter in a single-knife cutting are shown in Figure 17. Observation of the figure revealed that stem debris was lost from both the upper and lower incisions each time sugarcane was cut, with the loss of debris being more significant at the upper incision than at the lower. The lower surface of the stalk was relatively flat, while the upper surface was uneven. As the cutting blades continued to cut into the stalks, the upper stalk incision gradually increased in size and was accompanied by an upward trend. An axial crack appeared near the incision, as seen in the yellow box in the figure. The more and longer the crack appears, the more likely it is to increase the broken rate of sugarcane stalks. Due to the action of the beveled edge of the cutting blade, an angle is created at the incision, which increases the force on the incision and thus tends to cause tearing of the sugarcane stem.

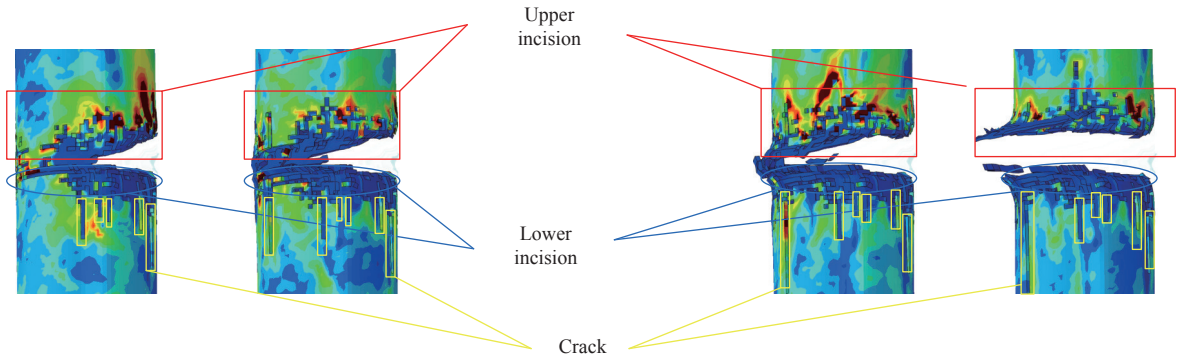

Figure 17 Analysis of the damaging effect of single-knife cutting

To deeply investigate the cutting effect of sugarcane stalks under multi-cutting, the initial position of the stalks and the cutter were adjusted and the effect of the stalks under the action of multi-cutting was analyzed, as shown in Figure 18. In the first cutting, the epidermis of the stalk was cut to form a slight edge. As the blade advances, it continues to cut along the edge, and the action of the second knife causes the edge to increase significantly, and so on, until the stalk is finally cut off, according to the stress cloud diagram of the multi-blade cutting in Figure 18. The minimum and maximum stress values during the cutting process of the first blade were 1.64 MPa and 8.24 MPa, respectively, and the maximum and minimum stresses of the second blade were 8.382 MPa and 1.023 MPa, respectively. During the cutting process, the rectangular blade used has a trapezoidal front end with no cutting edge, and the trapezoidal blade produces an impact cut on the stalk, resulting in the second half of the stalk being washed away.

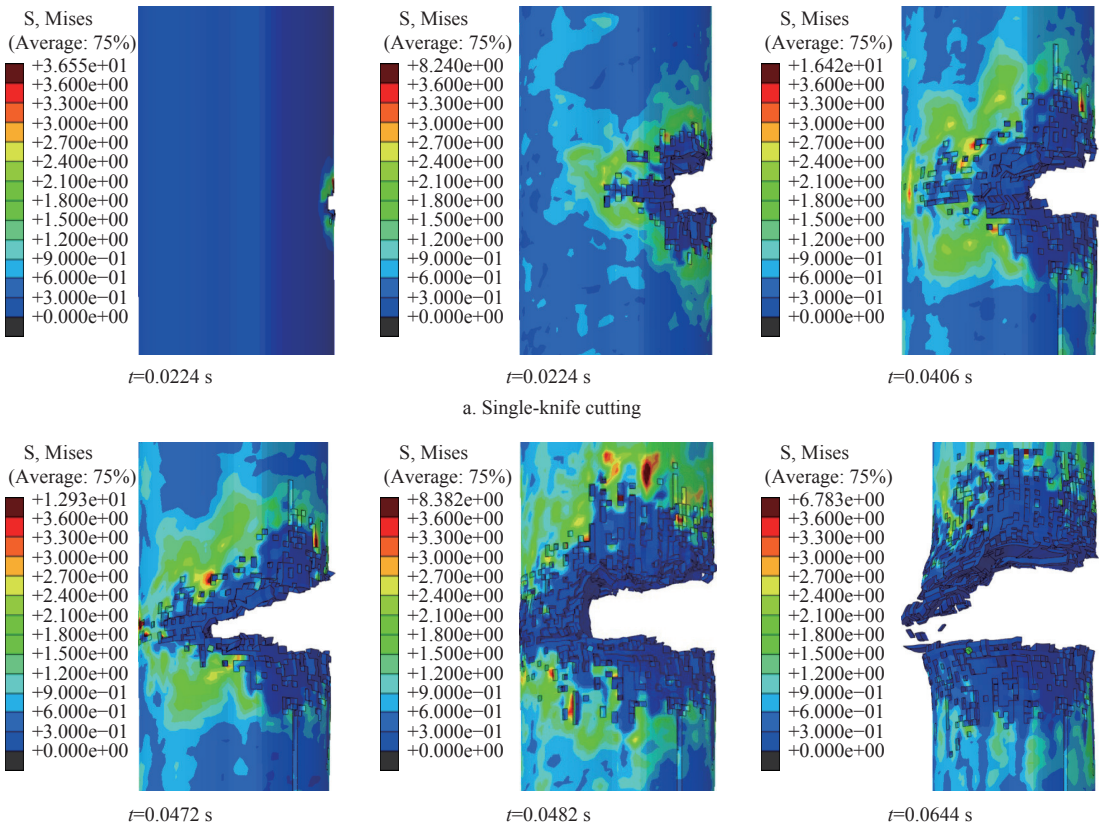

Figure 18 Changes in stem incision for different cutting methods

As seen in the stress change diagram, the stalks were subjected to multiple load impacts during the multi-cutter cutting process, and the tensile stress change was more significant, which was more likely to lead to sugarcane ratoon breakage. Compared with the first knife, the incision after the second knife cut lost more in the stem axis. During the multi-knife cutting process, the different cuts of the blades into the stalks made the axial contact surface of the stalks increase, resulting in lower shear and cutting forces and more stalk breakage. In addition, it is also easy to cause sugarcane ratoon breakage, tearing, or even splitting and bursting, thus increasing the broken rate of sugarcane ratoons. According to Figure 18d, it is evident that there are more splits on the stalks after cutting compared to the yellow box in Figure 17, which indicates that multi-cutting produces a higher broken rate of sugarcane ratoon than single-knife cutting and is more likely to result in the breakage of multiple ratoons.

6 Conclusions

1) The cutter is an essential part of the sugarcane harvester, the mathematical model of the double-disk cutter was established,

which came up with the general condition of no missed cuts of the cutter. Based on the secondary development module of ABAQUS software, the finite element model of sugarcane stalks with different anisotropy was established by using UMAT subroutine, and it was verified by bench shear test. The correlation coefficient R^2 of the two curves was 0.9621, which indicated that the established finite element model of sugarcane stalk is accurate and reliable in mechanical transfer.

2) The effects of blade inclination angle, blade rotational speed, and forward speed of the cutter on stalk cutting were analyzed, and the results showed that the magnitude of maximum shear force and maximum cutting force increased and then decreased with the increase of inclination angle. The maximum values were all at a blade inclination angle of 20°, with the maximum values of 133.1 N and 471.1 N. As the rotational speed of the cutter increases, the maximum shear force increases and then decreases with a maximum value of 128.26 N, while the maximum cutting force shows an increase and then a decrease and then an increase with a maximum value of 346.7 N. With the increase in the forward speed, the maximum shear force and the maximum cutting force on the sugarcane stalks showed a trend of increasing and decreasing. When the forward speed of the cutter reached 3.4 km/h, the maximum shear force and the maximum cutting force on sugarcane stalks reached the maximum values of 289.6 N and 1645.4 N, respectively; The orthogonal experiments results indicated that the optimal parameters for the cutter were under a combination with blade inclination angle of 11.3°, blade rotation speed of 659.3 r/min, and forward speed of 1.5 km/h. Under these conditions, the maximum shear and cutting forces were 305.1 N and 368.1 N, respectively. Moreover, the transmission of stress waves in sugarcane was investigated, and the results explained the damage mechanism of the stalk in the cutting process and effectively predicted the damage location of the stalk. In addition, changes in sugarcane ratoon stem openings after multiple and single-knife cuts were analyzed and it was found that multi-cutting produced more significant damage and were more likely to increase sugarcane ratoons' breakage rate.

Acknowledgments

This work was financially supported by the Anhui Province Agricultural Machinery and Equipment Application Industry Technology System Project, the School-Level Cross-Disciplinary Project (Grant No. XK-XJJC002) and the Project of Talent Introduction of Anhui Science and Technology University: Research on Dynamic Characteristics of Double Disc Cutter and Analysis of Stalk Breaking Mechanisms (Grant No. JXYJ202201).

[References]

[1] Arjona E, Bueno G, Salazar L. An activity simulation model for the analysis of the harvesting and transportation systems of a sugarcane plantation. Computers and Electronics in Agriculture, 2001; 32(3): 247–264.

[2] Santoro E, Soler E M, Cherri A C. Route optimization in mechanized sugarcane harvesting. Computers and Electronics in Agriculture, 2017; 141: 140–146.

[3] Xie D B, Chen L, Liu L C, Chen L Q, Wang H. Actuators and sensors for application in agricultural robots: A review. Machines, 2022; 10(10): 913.

[4] Bai J, Ma S C, Wang F L, Xing H N, Ma J Z, Hu J W. Field test and evaluation on crop dividers of sugarcane chopper harvester. Int J Agric & Biol Eng, 2021; 14(1): 118–122.

[5] Liu X P, Niu Z J, Li M, Hou M X, Wei L J, Zhang Y, et al. Design and experimental research on disc-type seeding device for single-bud sugarcane seeds. Int J Agric & Biol Eng, 2023; 16(2): 115–124.

[6] Wang F L, Zhang W H, Di M L, Wu X H, Song Z H, Xie B, et al. Sugarcane cutting quality using contra-rotating basecutters. Transactions of the ASABE, 2019; 62(3): 737–747.

[7] Momin M A, Wempe P A, Grift T E, Hansen A C. Effects of four base cutter blade designs on sugarcane stem cut quality. Transactions of the ASABE, 2017; 60(5): 1551–1560.

[8] Xie L X, Wang J, Cheng S M, Zeng B S, Yang Z Z. Performance evaluation of a chopper system for sugarcane harvester. Sugar Tech, 2019; 21(5): 825–837.

[9] Mo H N, Li S P, Zhou J H, Zeng B, He G Q, Qiu C. Simulation and experimental investigations on the sugarcane cutting mechanism and effects of influence factors on the cutting quality of small sugarcane harvesters under vibration excitations. Mathematical Problems in Engineering, 2022; 2022: 1–28.

[10] Li Z, Lin Z L, Li S Y, Zhang H. Optimization research on the working parameters of sugarcane harvester on the cutting time of stalks using virtual prototype technology. Sugar Tech, 2023; 25(1): 41–56.

[11] Bai J, Ma S C, Ke W L, Wang F L, Xing H N, Ma J Z, et al. Experimental research on sugarcane under-the-ground basecutting. Applied Engineering in Agriculture, 2020; 36(3): 331–339.

[12] Mathanker S K, Grift T E, Hansen A C. Effect of blade oblique angle and cutting speed on cutting energy for energycane stems. Biosystems Engineering, 2015; 133: 64–70.

[13] Wang F L, Ma S C, Xing H N, Bai J, Ma J, Wang M L. Effect of contra-rotating basecutter parameters on basecutting losses. Sugar Tech, 2021; 23(2): 278–285.

[14] Rashvand M, Altieri G, Genovese F, Li Z G, Di Renzo G C. Numerical simulation as a tool for predicting mechanical damage in fresh fruit. Post-harvest Biology and Technology, 2022; 187: 111875.

[15] Wang T, Liu Z D, Yan X L, Mi G P, Liu S Y, Chen K Z, et al. Finite element model construction and cutting parameter calibration of wild chrysanthemum stem. Agriculture-Basel, 2022; 12(6): 894.

[16] Niu Z J, Xu Z, Deng J T, Zhang J, Pan S J, Mu H T. Optimal vibration parameters for olive harvesting from finite element analysis and vibration tests. Biosystems Engineering, 2022; 215: 228–238.

[17] Liu H J, Han X W, Fadiji T, Li Z, Ni J. Prediction of the cracking susceptibility of tomato pericarp: Three-point bending simulation using an extended finite element method. Post-harvest Biology and Technology, 2022; 187: 111876.

[18] Xie L X, Wang J, Cheng S M, Zeng B S, Yang Z Z. Optimisation and finite element simulation of the chopping process for chopper sugarcane harvesting. Biosystems Engineering, 2018; 175: 16–26.

[19] Qiu M M, Meng Y M, Li Y Z, Shen X B. Sugarcane stem cut quality investigated by finite element simulation and experiment. Biosystems Engineering, 2021; 206: 135–149.

[20] Wang Q Q, Zhang Q W, Zhang Y, Zhou G A, Li Z Q, Chen L Q. Lodged sugarcane/crop dividers interaction: analysis of robotic sugarcane harvester in agriculture via a rigid-flexible coupled simulation method. Actuators, 2022; 11(1): 23.

[21] Dai J P, Huang J K, Chen L H, Ji J N, Li J. Three-dimensional constitutive relation of the root-soil composite using homogenization theory. Transactions of the CSAE, 2022; 38(13): 76–83. (in Chinese)

[22] Xie L X, Wang J, Cheng S M, Zeng B S, Yang Z Z. Optimisation and dynamic simulation of a conveying and top breaking system for whole-stalk sugarcane harvesters. Biosystems Engineering, 2020; 197: 156–169.

[23] Huang H D, Wang Y X, Tang Y Q, Zhao F, Kong X F. Finite element simulation of sugarcane cutting. Transactions of the CSAE, 2011; 27(2): 161–166. (in Chinese)

[24] Mello R D C, Harris H. Hogarth D M. Cane damage and mass losses for conventional and serrated basecutter blades. Proc Aust Soc Sugar Cane Tech, 2000; 6: 84–91.

[25] Luo Y Q, Ren Y H, Zhou Z X, Huang X M, Song T J. Prediction of single-tooth sawing force based on tooth profile parameters. International Journal of Advanced Manufacturing Technology, 2016; 86(1-4): 641–650.

[26] Zhou Y, Qu Y G, Mo Z F. Design and experiment of oblique cutting and feeding device for sugarcane. Transactions of the CSAE, 2012; 28(14): 17–23. (in Chinese)

[27] Yang W, Zhao W J, Liu Y D, Chen Y Q, Yang J. Simulation of forces acting on the cutter blade surfaces and root system of sugarcane using FEM and SPH coupled method. Computers and Electronics in Agriculture, 2021; 180: 105893.

[28] Do T V, Pham T M, Hao H. Stress wave propagation and structural response of precast concrete segmental columns under simulated blast loads. International Journal of Impact Engineering, 2020; 143: 103595.